NASA TM X-769

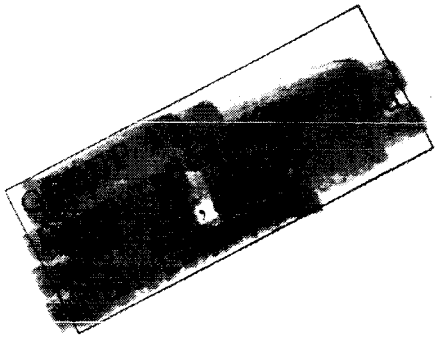

NASA TM X-769

TECHNICAL MEMORANDUM

X-769

WIND-TUNNEL MEASUREMENTS OF SOME DYNAMIC STABILITY CHARACTERISTICS OF 0.055-SCALE MODELS OF PROPOSED APOLLO COMMAND MODULE AND LAUNCH-ESCAPE CONFIGURATIONS AT MACH NUMBERS FROM 2.40 TO 4.65

By Robert A. Kilgore and Benjamin T. Averett

Langley Research Center
Langley Station, Hampton, Va.

NATIONAL AERONAUTICS AND SPACE ADMINISTRATION
WASHINGTON
March 1963

NATIONAL AERONAUTICS AND SPACE ADMINISTRATION

TECHNICAL MEMORANDUM X-769

WIND-TUNNEL MEASUREMENTS OF SOME DYNAMIC STABILITY CHARACTERISTICS OF 0.055-SCALE MODELS OF PROPOSED APOLLO COMMAND MODULE AND LAUNCH-ESCAPE CONFIGURATIONS AT MACH NUMBERS FROM 2.40 TO 4.65*

By Robert A. Kilgore and Benjamin T. Averett

SUMMARY

Wind-tunnel measurements of some of the dynamic stability characteristics of 0.055-scale models of proposed Apollo configurations identified as $ET_{12}C$, $E_4T_{12}C$, and C have been made at Mach numbers from 2.40 to 4.65 by using a forced-oscillation technique. Damping in pitch and oscillatory longitudinal stability were measured for the launch-escape configurations $ET_{12}C$ and $E_4T_{12}C$ and the command module C with the heat shield aft and in a reentry attitude. Damping in yaw and oscillatory directional stability were measured for the command module in a reentry attitude. Tests were made at angles of attack likely to be encountered during the several phases of flight.

The addition of toroidal tanks to the escape rocket of the model of the launch-escape configuration increased the stability in pitch and decreased the damping in pitch near a mean angle of attack α of 0°.

The model of the command module with the heat shield aft had positive damping in pitch and positive oscillatory longitudinal stability for all test conditions. The damping in pitch of the model of the command module in a reentry attitude was slightly positive except for data taken at the lower Reynolds numbers at the higher Mach numbers. The stability in pitch varied almost directly with α from unstable near $\alpha = 134^\circ$ to stable near $\alpha = 158^\circ$, with zero stability occurring near $\alpha = 140^\circ$. The damping in yaw for the model of this configuration was generally positive. The stability in yaw increased slightly with angle of attack.

---

* Title, Unclassified.

INTRODUCTION

A research program is being conducted by the National Aeronautics and Space Administration to determine the aerodynamic characteristics of proposed configurations of the Project Apollo vehicle, a manned lunar-exploration spacecraft. Wind-tunnel measurements of the static longitudinal aerodynamic characteristics of 0.07-scale models of proposed configurations of the Project Apollo vehicle are presented for Mach numbers from 1.57 to 4.65 in reference 1 and from Mach numbers of 0.30 to 1.20 in reference 2.

This paper presents without detailed analysis some of the dynamic stability characteristics of 0.055-scale models of proposed reentry and launch-escape configurations of the Apollo command module as obtained in the Langley Unitary Plan wind tunnel at Mach numbers from 2.40 to 4.65. The dynamic stability characteristics in pitch of the launch-escape configurations $ET_{12}C$ and $E_4T_{12}C$ and the command module C with the heat shield aft and in a reentry attitude were measured. In addition, the dynamic stability characteristics in yaw for the command module in a reentry attitude were measured. The model of the launch-escape configuration had no provision for an investigation of the effect of escape-rocket thrust or exhaust on the dynamic stability characteristics. A limited range of Reynolds number was investigated to determine the effect of Reynolds number on the stability characteristics. The data are presented for the angle-of-attack ranges likely to be encountered during the several phases of flight.

SYMBOLS

The aerodynamic parameters are referred to the body system of axes originating at the oscillation centers of the models as shown in figure 1. The symbols used herein are defined as follows:

A	reference area, $\pi\left(\frac{d}{2}\right)^2$, 0.3912 sq ft
d	reference length, maximum diameter of model, 0.7058 ft
k	reduced-frequency parameter, $\frac{\omega d}{V}$, radians
M	free-stream Mach number
q	pitching velocity, radians/sec
q_∞	free-stream dynamic pressure, lb/sq ft
R	Reynolds number based on d
r	yawing velocity, radians/sec

V free-stream velocity, ft/sec

α mean angle of attack, deg or radians

β angle of sideslip, radians

ω angular velocity, 2π(Frequency of oscillation), radians/sec

C_m pitching-moment coefficient, $\frac{\text{Pitching moment}}{q_\infty Ad}$

C_n yawing-moment coefficient, $\frac{\text{Yawing moment}}{q_\infty Ad}$

$C_{m_\alpha} = \frac{\partial C_m}{\partial \alpha}$ per radian

$C_{m_q} = \frac{\partial C_m}{\partial \left(\frac{qd}{V}\right)}$ per radian

$C_{n_\beta} = \frac{\partial C_n}{\partial \beta}$ per radian

$C_{n_r} = \frac{\partial C_n}{\partial \left(\frac{rd}{V}\right)}$ per radian

$C_{m_{\dot{\alpha}}} = \frac{\partial C_m}{\partial \left(\frac{\dot{\alpha}d}{V}\right)}$ per radian

$C_{m_{\dot{q}}} = \frac{\partial C_m}{\partial \left(\frac{\dot{q}d^2}{V^2}\right)}$ per radian

$C_{n_{\dot{\beta}}} = \frac{\partial C_n}{\partial \left(\frac{\dot{\beta}d}{V}\right)}$ per radian

$C_{n_{\dot{r}}} = \frac{\partial Cn}{\partial \left(\frac{\dot{r}d^2}{V^2}\right)}$ per radian

The equations used to obtain the following aerodynamic parameters are presented in the section entitled "Reduction of Data."

$C_{m_q} + C_{m_{\dot{\alpha}}}$ damping-in-pitch parameter, per radian

$C_{m_\alpha} - k^2 C_{m_{\dot{q}}}$ oscillatory-longitudinal-stability parameter, per radian

$C_{n_r} - C_{n_{\dot{\beta}}} \cos \alpha$ damping-in-yaw parameter, per radian

$C_{n_\beta} \cos \alpha + k^2 C_{n_{\dot{r}}}$ oscillatory-directional-stability parameter, per radian

A dot over a quantity denotes a derivative with respect to time.

MODELS

Design dimensions of 0.055-scale models of the proposed Apollo launch-escape configurations $ET_{12}C$ and $E_4T_{12}C$ and of the command module C are shown in figure 1. The designations used were assigned by the prime contractor for Apollo to facilitate identification of various configurations under investigation. The letters are associated with the component parts as follows: E is for the escape rocket, T for the tower, and C for the command module. Numbered subscripts refer to specific versions of each component.

The models were made of aluminum, with the escape-rocket tower made of steel and the escape-rocket motor made of magnesium and plastic-impregnated fiber glass. The toroidal tanks on the escape rocket were removable. The model surfaces exposed to the airstream were aerodynamically smooth. The openings in the models necessary for sting clearance are also shown in figure 1.

Because of tunnel size and balance load limitations, the size of the models was restricted and the centers of oscillation were not coincident with the proposed center-of-mass locations for the model of the launch-escape configuration and the model of the command module in a reentry attitude. The oscillation center was not at the proposed center-of-mass location for the model of the command module with the heat shield aft because no provision was made for moving the model forward on the oscillating balance when the escape-rocket motor and tower were removed. In order to provide the desired angle-of-attack range, the models were mounted at fixed offset angles with respect to the center line of the oscillating balance as shown in figure 1.

TUNNEL

Tests were made in the high Mach number test section of the Langley Unitary Plan wind tunnel, which is a variable pressure, continuous-flow tunnel. The nozzle leading to the 4- by 4-foot test section is of the asymmetric sliding-block type and permits a continuous variation of test-section Mach number from approximately 2.3 to 4.7.

The sting system is supported by a horizontal strut extending from wall to wall downstream of the test section. For these tests the models were rotated 90°

on the sting so that the angle-of-attack range was obtained in the horizontal plane. The sting-support strut is capable of an angle-of-attack range from -8° to 17° when used in conjunction with the forced-oscillation mechanism. A complete description of the tunnel is given in reference 3.

APPARATUS AND PROCEDURE

The models are mounted on an oscillation balance which is forced to perform an essentially sinusoidal, single-degree-of-freedom motion of 2° amplitude. A motor-driven Scotch yoke arrangement provides the oscillatory motion and allows accurate control of oscillation frequencies from about 2 to 25 cycles per second. A detailed description of the oscillation mechanism is given in reference 4. A photograph of the Apollo launch-escape configuration $ET_{12}C$ mounted on the oscillation mechanism in the tunnel test section is presented as figure 2.

Dynamic data are obtained from the oscillation balance by alternating-current strain-gage bridges which sense the instantaneous torque required to drive the model and the instantaneous angular displacement of the model with respect to the sting. These strain-gage bridges modulate 3,000-cycle carrier voltages which are passed through coupled electrical sine-cosine resolvers that rotate at the frequency of oscillation of the model. The resolvers divide the signals into orthogonal components, which are then demodulated and read on damped digital voltmeters. By responding only to signals at the fundamental frequency of oscillation, the resolver and damped-voltmeter system performs the desirable function of eliminating the effects of random torque inputs due to airstream turbulence or buffeting. The maximum torque required to drive the model, the maximum displacement of the model with respect to the sting, and the phase angle between torque and displacement are found from the orthogonal components of torque and displacement. The frequency of oscillation is obtained by counting pulses generated by an induction-coil pickup and a 100-tooth gear fastened to the shaft of one of the resolvers. The damping and spring-inertia characteristics are then computed from the measured values of torque, displacement, phase angle, and frequency.

REDUCTION OF DATA

For the pitching tests, measurements were made of the maximum applied pitching moment M_Y, the maximum angular displacement in pitch of the model with respect to the sting Θ, the phase angle η between M_Y and Θ, and the angular velocity of the forced oscillation ω.

As explained in detail in reference 5, the damping coefficient for this single-degree-of-freedom system can be computed as

$$C_Y = \frac{M_Y \sin \eta}{\omega \Theta} \tag{1}$$

and the spring-inertia characteristic can be computed as

$$K_Y - I_Y \omega^2 = \frac{M_Y \cos \eta}{\Theta} \tag{2}$$

where K is the torsional spring constant of the system and I is the inertia of the system about the axis indicated by the subscript.

The damping-in-pitch parameter was computed as

$$C_{m_q} + C_{m_{\dot{\alpha}}} = -\frac{V}{q_\infty A d^2}\left[\left(\frac{M_Y \sin \eta}{\omega\Theta}\right)_{\text{wind on}} - \left(\frac{M_Y \sin \eta}{\omega\Theta}\right)_{\text{wind off}}\right] \tag{3}$$

and the oscillatory-longitudinal-stability parameter was computed as

$$C_{m_\alpha} - k^2 C_{m_{\dot{q}}} = -\frac{1}{q_\infty A d}\left[\left(\frac{M_Y \cos \eta}{\Theta}\right)_{\text{wind on}} - \left(\frac{M_Y \cos \eta}{\Theta}\right)_{\text{wind off}}\right] \tag{4}$$

The wind-off value of $\frac{M_Y \sin \eta}{\omega\Theta}$ was determined at the frequency of wind-off velocity resonance. The wind-off and wind-on values of $\frac{M_Y \cos \eta}{\Theta}$ were determined at the same value of ω^2.

For the yawing tests, measurements were made of the maximum applied yawing moment M_Z, the maximum angular displacement in yaw of the model with respect to the sting Ψ, the phase angle λ between M_Z and Ψ, and the angular velocity of the forced oscillation ω.

The system characteristics in yaw were computed as

$$C_Z = \frac{M_Z \sin \lambda}{\omega\Psi} \tag{5}$$

and

$$K_Z - I_Z\omega^2 = \frac{M_Z \cos \lambda}{\Psi} \tag{6}$$

The damping-in-yaw parameter was computed as

$$C_{n_r} - C_{n_{\dot{\beta}}} \cos \alpha = -\frac{V}{q_\infty A d^2}\left[\left(\frac{M_Z \sin \lambda}{\omega\Psi}\right)_{\text{wind on}} - \left(\frac{M_Z \sin \lambda}{\omega\Psi}\right)_{\text{wind off}}\right] \tag{7}$$

and the oscillatory-directional-stability parameter was computed as

$$C_{n_\beta} \cos \alpha + k^2 C_{n_{\dot{r}}} = +\frac{1}{q_\infty A d}\left[\left(\frac{M_Z \cos \lambda}{\Psi}\right)_{\text{wind on}} - \left(\frac{M_Z \cos \lambda}{\Psi}\right)_{\text{wind off}}\right] \tag{8}$$

As for the pitching-oscillation tests the wind-off value of $\frac{M_Z \sin \lambda}{\omega \Psi}$ was determined at the frequency of wind-off velocity resonance and the wind-off and wind-on values of $\frac{M_Z \cos \lambda}{\Psi}$ were determined at the same value of ω^2.

No factor of 2 appears in equations (3) and (7) because the reduced-frequency parameter is defined as $k = \frac{\omega d}{V}$. The expression $\cos \alpha$ appears in the damping-in-yaw and oscillatory-directional-stability parameters because these terms are expressed in the body system of axes.

TESTS AND PRESENTATION OF DATA

The tests were made at Mach numbers from 2.40 to 4.65 and at Reynolds numbers, based on the maximum diameter of the model, from 1.05×10^6 to 3.39×10^6. The upper values of Reynolds number were dictated by the electrical power available for the tunnel drive system.

The data were taken for angles of attack likely to be encountered during the several phases of flight. ($\alpha = 0$ corresponds to heat shield aft on the command module.) Bow-shock reflections from the side walls of the tunnel limited the range of angle of attack at which valid data could be obtained. All data affected by shock reflections have been omitted from this paper.

Dynamic stability data obtained in this investigation are presented in the following figures:

Configuration	M	R	α, deg	Figure
Longitudinal				
$ET_{12}C$ (launch escape, toroidal tanks on)	2.40 2.98 3.96 4.65	1.58×10^6 1.67 2.09 2.69	-12 to 6 -12 to 6 -12 to 6 -12 to 6	3(a) 3(b) 3(c) 3(d)
$E_4T_{12}C$ (launch escape, toroidal tanks off)	2.40 2.98 3.96 4.65 4.65	1.58×10^6 1.67 2.09 2.69 1.07	-8 to 4 -8 to 4 -8 to 4 -8 to 4 -8 to 4	3(a) 3(b) 3(c) 3(d) 3(d)
C (command module) heat shield aft	2.40 2.98 3.96 4.65	1.58×10^6 1.68 2.09 2.69	-14 to 6 -14 to 6 -14 to 6 -14 to 6	4 4 4 4
C (command module) reentry attitude	2.40 2.40 2.98 3.96 3.96 4.65 4.65 4.65	1.05×10^6 1.58 1.68 1.08 2.09 1.07 2.69 3.39	136 to 158 141 to 158 138 to 158 135 to 158 135 to 158 135 to 156 133 to 158 133 to 158	5(a) 5(a) 5(b) 5(c) 5(c) 5(d) 5(d) 5(d)
Directional				
C (command module) reentry attitude	2.40 2.98 3.96 4.65	1.58×10^6 1.68 2.09 2.69	138 to 158 138 to 158 136 to 158 133 to 158	6 6 6 6

Positive damping in pitch and positive stability in pitch are indicated by negative values of $C_{m_q} + C_{m_{\dot{\alpha}}}$ and $C_{m_\alpha} - k^2 C_{m_{\dot{q}}}$. Positive damping in yaw is indicated by negative values of $C_{n_r} - C_{n_{\dot{\beta}}} \cos \alpha$ but positive stability in yaw is indicated by positive values of $C_{n_\beta} \cos \alpha + k^2 C_{n_{\dot{r}}}$.

Typical schlieren photographs of the models are presented as figures 7 to 10. Since angle of attack was obtained in the horizontal plane with the models rotated 90° on the balance, these photographs are, in effect, taken from above the models mounted at the angles of attack indicated in these figures.

ANALYSIS AND SUMMARY OF RESULTS

As seen in figure 3, the addition of the toroidal tanks to the escape rocket of the model of the launch-escape configuration increased the stability in pitch and decreased the damping in pitch near $\alpha = 0°$ for all Mach numbers. Certain data, identified by flagged symbols, were taken at frequencies other than the frequency necessary for velocity resonance of the model. This limited amount of data indicates no pronounced effect of reduced frequency on the dynamic characteristics. A reduction in Reynolds number by a factor of 2.5 had little effect on the dynamic characteristics at $M = 4.65$ as can be seen in figure 3(d).

The data presented in figure 4 indicate that the model of the command module with the heat shield aft has positive damping in pitch and positive oscillatory longitudinal stability for all test conditions. The levels of damping and stability exhibited only slight dependence upon either Mach number or mean angle of attack.

The damping in pitch of the model of the command module in a reentry attitude is generally independent of mean angle of attack, as shown by the data of figure 5. The damping in pitch is slightly positive except at the lower Reynolds numbers at the higher Mach numbers where zero or slightly negative damping was measured. The stability in pitch varies almost directly with mean angle of attack α from unstable near $\alpha = 134°$ to stable near $\alpha = 158°$, with zero stability occurring near $\alpha = 140°$. A slight Reynolds number effect is noted at the higher Mach numbers. The damping in yaw for this configuration is generally slightly positive as shown in figure 6. The stability in yaw increases slightly from $\alpha = 134°$ to $\alpha = 158°$ with increased stability at the higher Mach numbers through the angle-of-attack range.

Some comparison of the flow around the configurations tested may be obtained from the schlieren photographs in figures 7 to 10.

Langley Research Center,
National Aeronautics and Space Administration,
Langley Station, Hampton, Va., December 5, 1962.

REFERENCES

1. Morgan, James R., and Fournier, Roger H.: Static Longitudinal Aerodynamic Characteristics of a 0.07-Scale Model of a Proposed Apollo Spacecraft at Mach Numbers of 1.57 to 4.65. NASA TM X-603, 1961.

2. Pearson, Albin O.: Wind-Tunnel Investigation of the Static Longitudinal Aerodynamic Characteristics of Models of Reentry and Atmospheric-Abort Configurations of a Proposed Apollo Spacecraft at Mach Numbers From 0.30 to 1.20. NASA TM X-604, 1961.

3. Anon.: Manual for Users of the Unitary Plan Wind Tunnel Facilities of the National Advisory Committee for Aeronautics. NACA, 1956.

4. Bielat, Ralph P., and Wiley, Harleth G.: Dynamic Longitudinal and Directional Stability Derivatives for a 45° Sweptback-Wing Airplane Model at Transonic Speeds. NASA TM X-39, 1959.

5. Braslow, Albert L., Wiley, Harleth G., and Lee, Cullen Q.: A Rigidly Forced Oscillation System for Measuring Dynamic-Stability Parameters in Transonic and Supersonic Wind Tunnels. NASA TN D-1231, 1962.

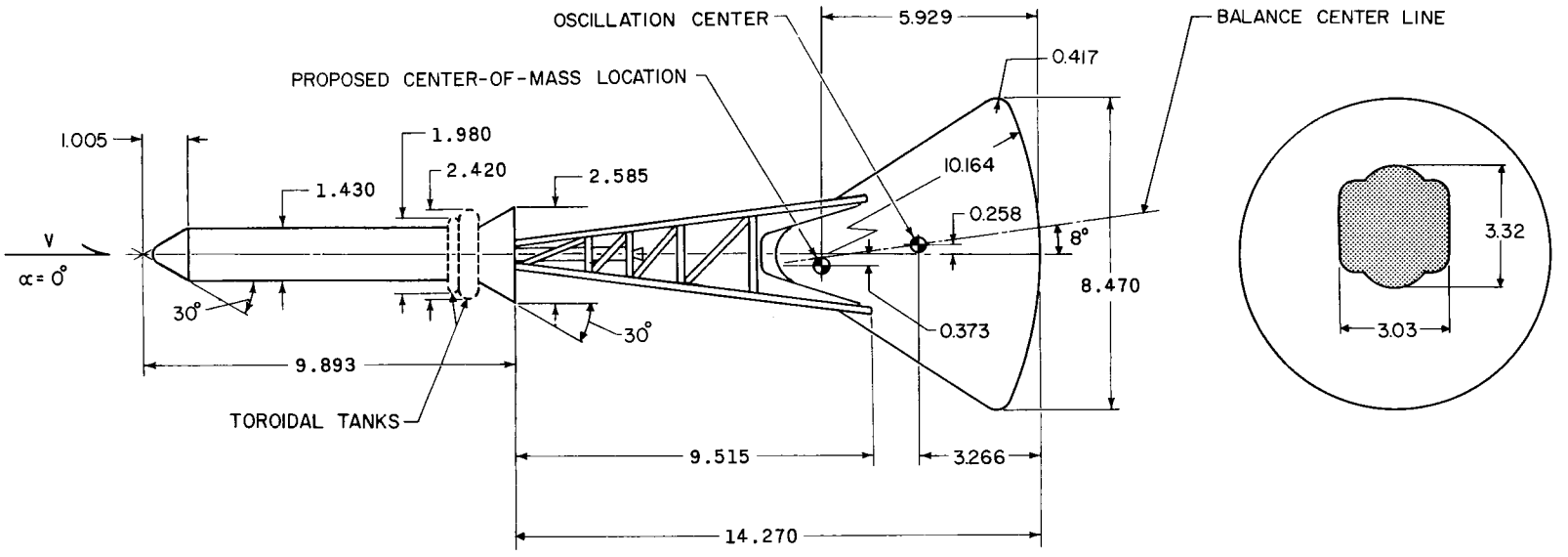

(a) Apollo launch-escape configuration $E_4T_{12}C$. With toroidal tanks, this is configuration $ET_{12}C$.

Figure 1.- Sketches of models tested, showing design dimensions. Openings in models for sting clearance are indicated by shaded portions. All linear dimensions are in inches.

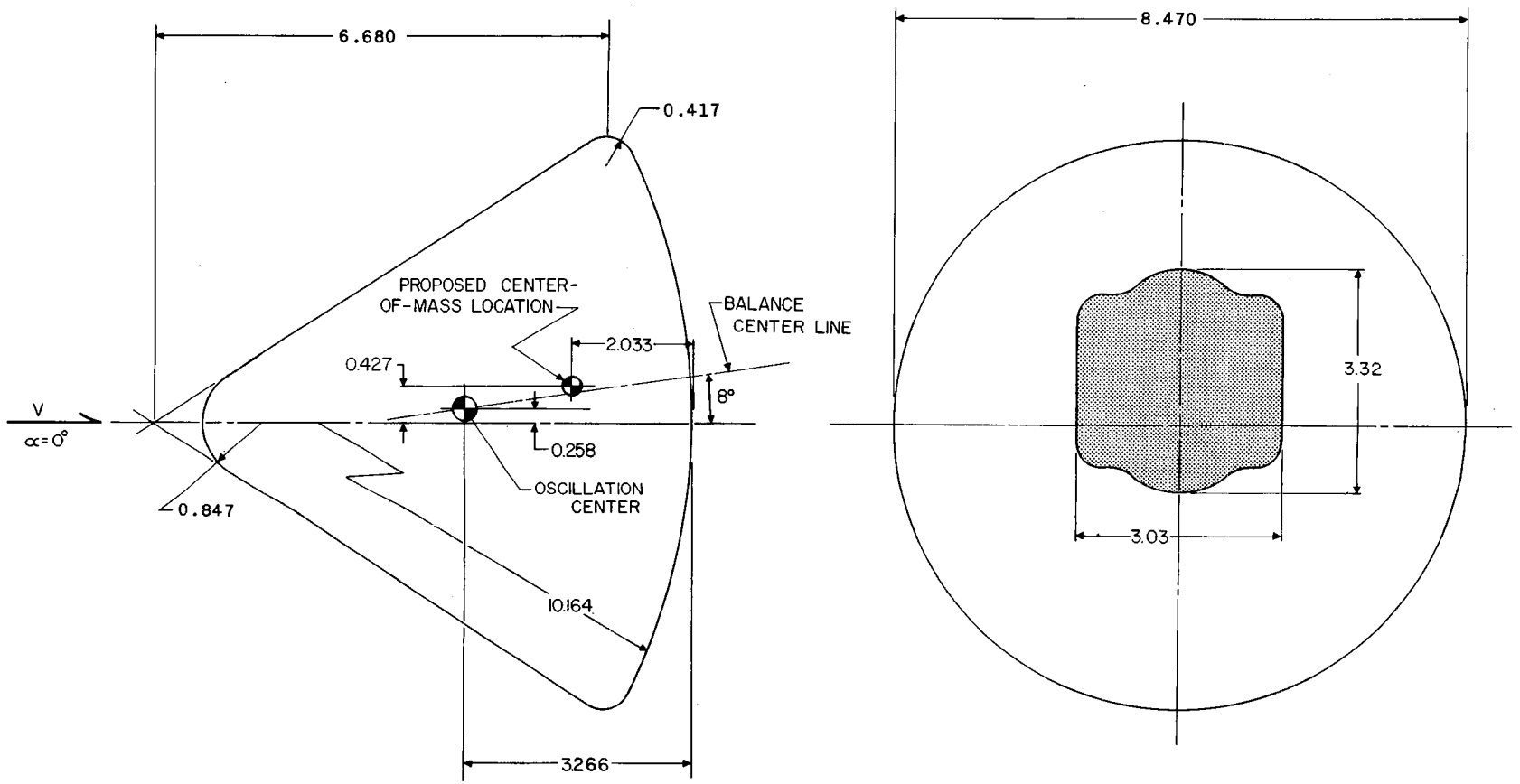

(b) Apollo command module C with heat shield aft.

Figure 1.- Continued.

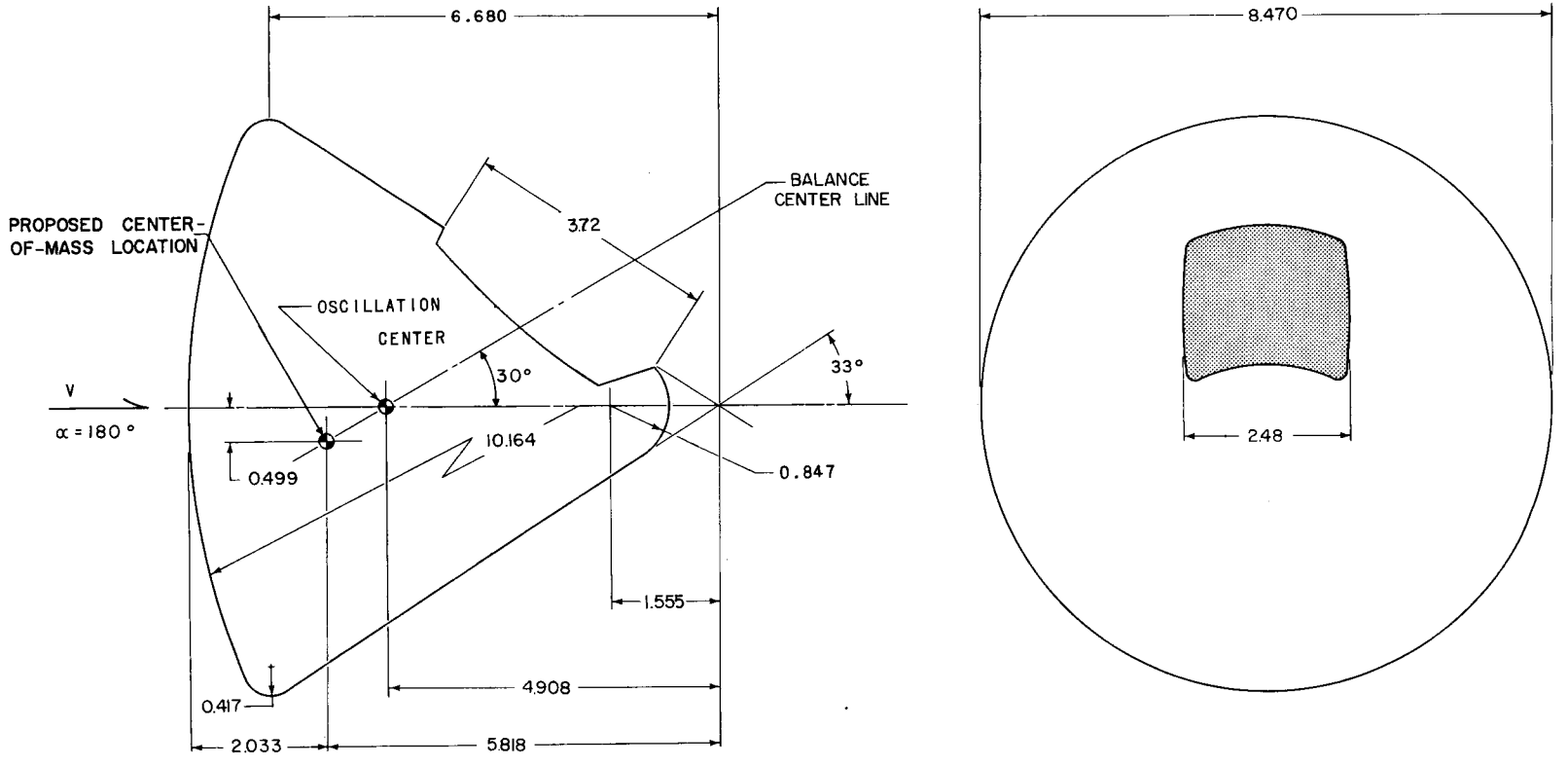

(c) Apollo command module C in a reentry attitude.

Figure 1.- Concluded.

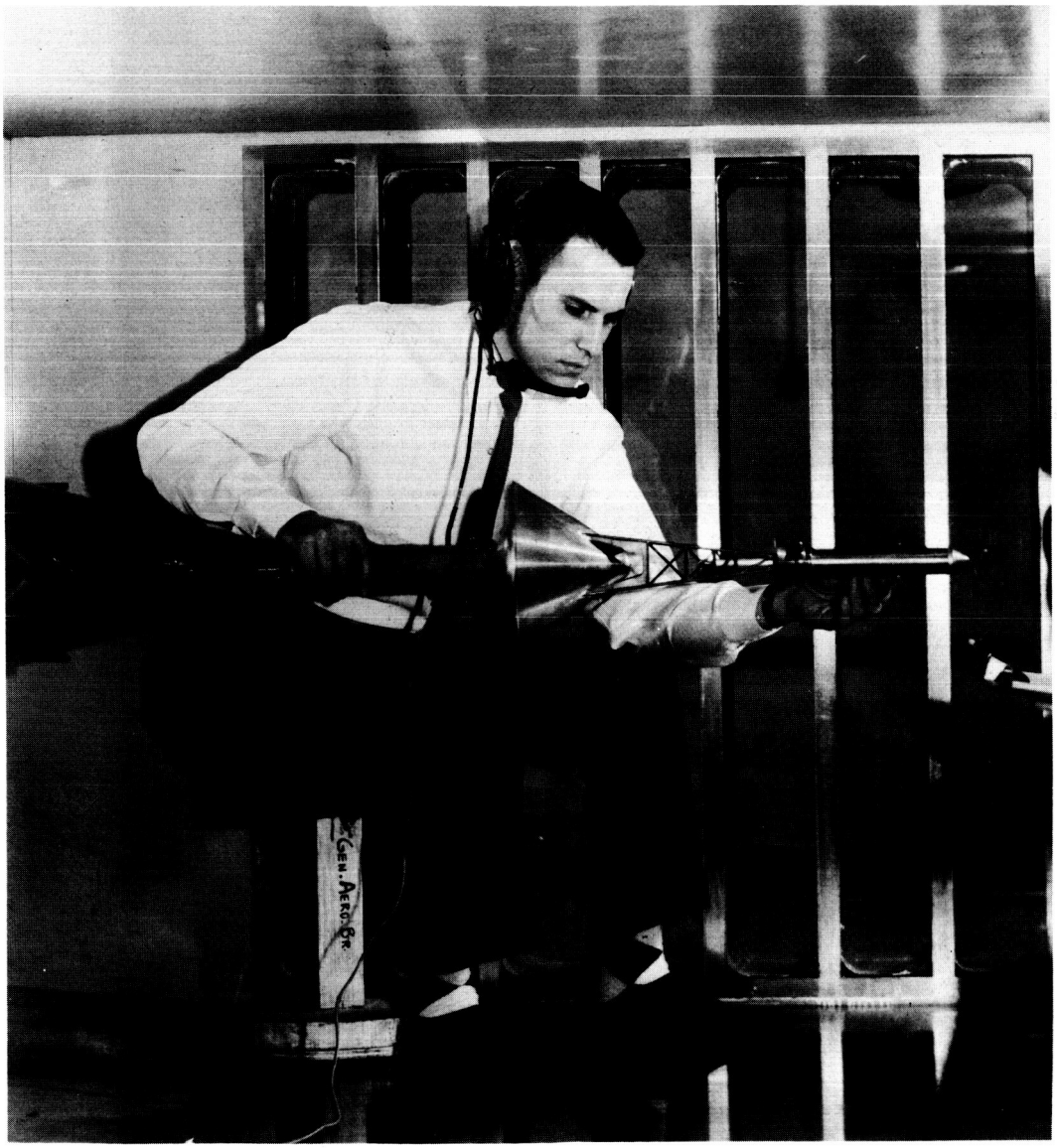

L-62-7075

Figure 2.- Model of Apollo launch-escape configuration $ET_{12}C$ mounted on oscillation mechanism in tunnel test section.

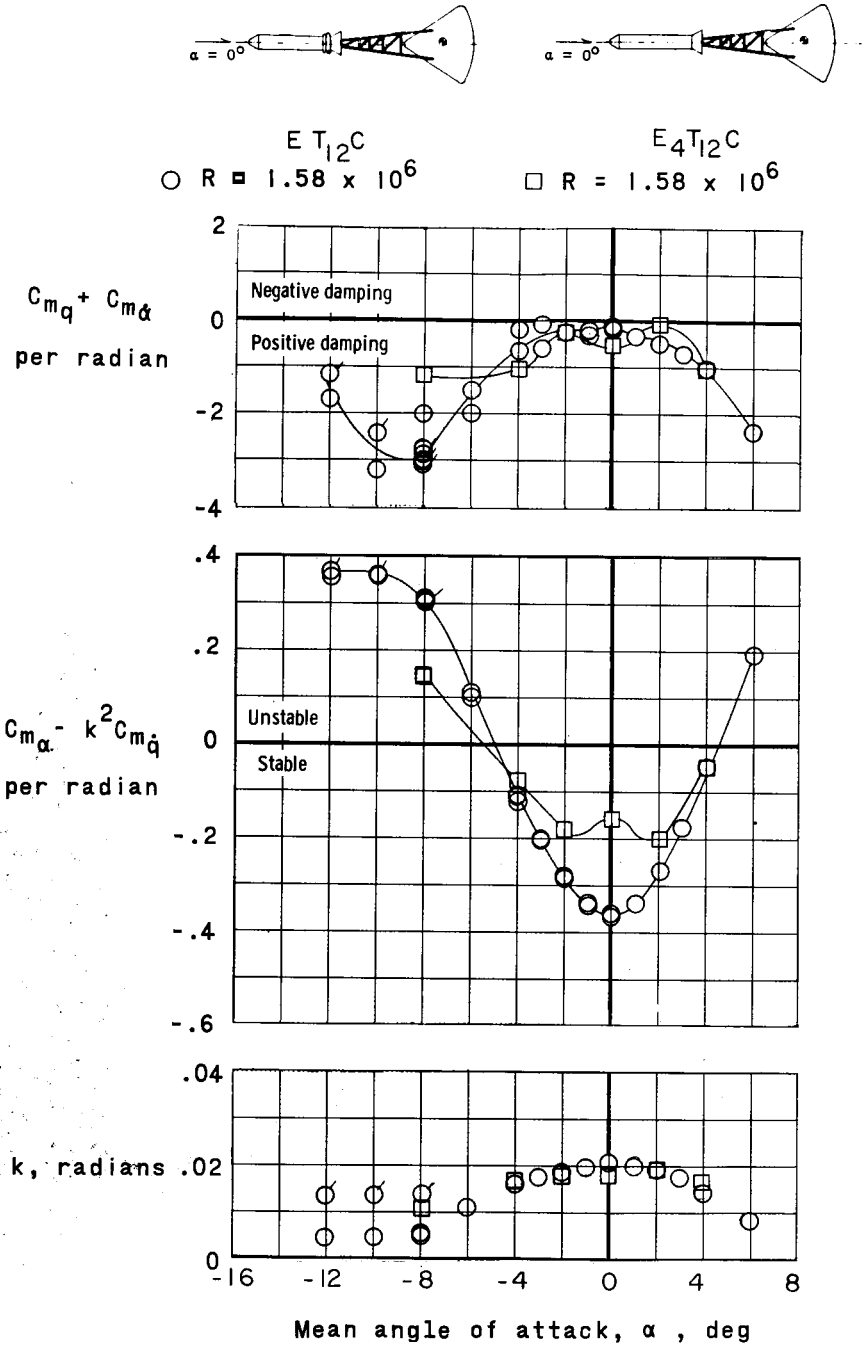

(a) M = 2.40.

Figure 3.- Variation of damping-in-pitch parameter, oscillatory-longitudinal-stability parameter, and reduced-frequency parameter with mean angle of attack α for models of launch-escape configurations $ET_{12}C$ and $E_4T_{12}C$. Flagged symbols indicate data taken at frequencies other than the frequency for velocity resonance of the model system.

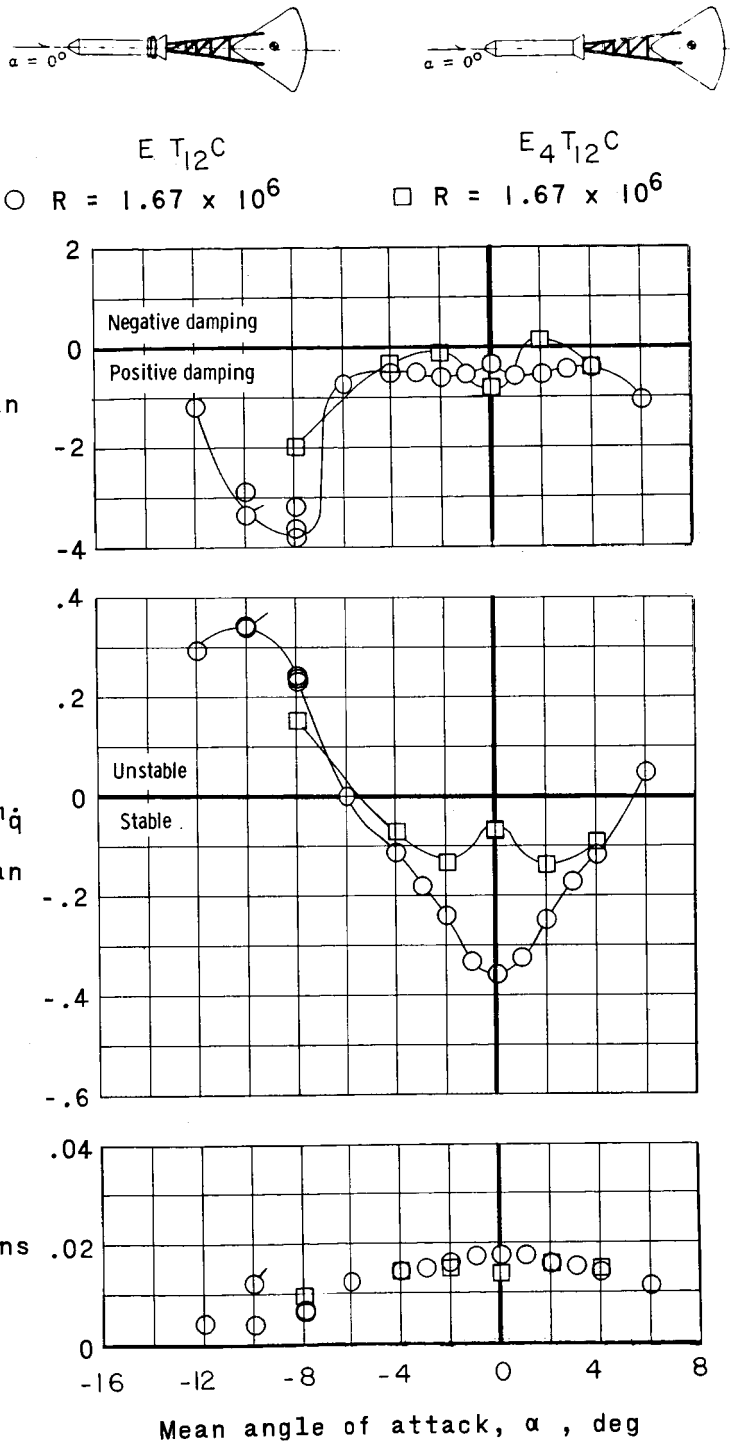

(b) M = 2.98.

Figure 3.- Continued.

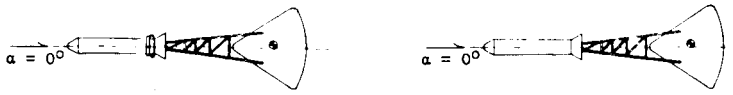

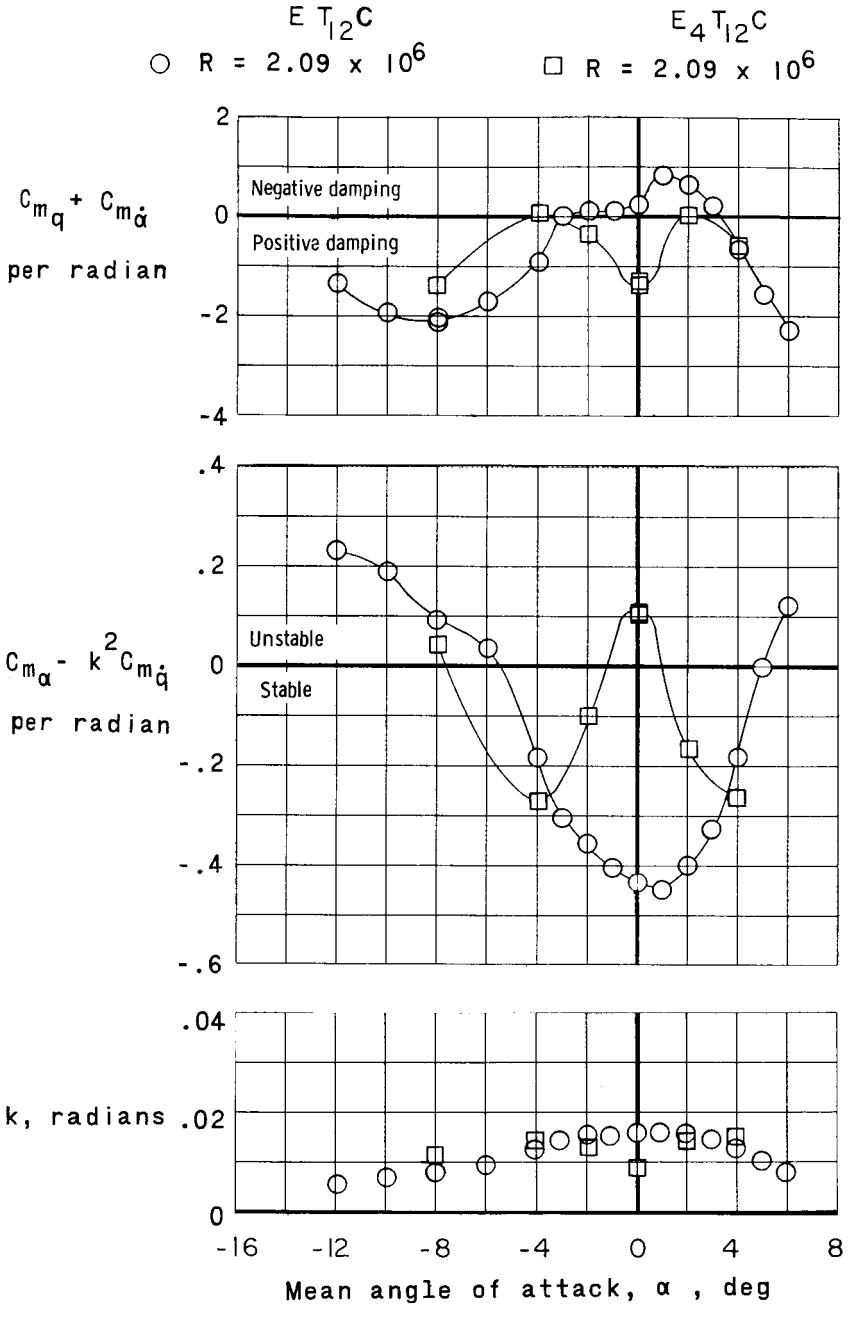

(c) M = 3.96.

Figure 3.- Continued.

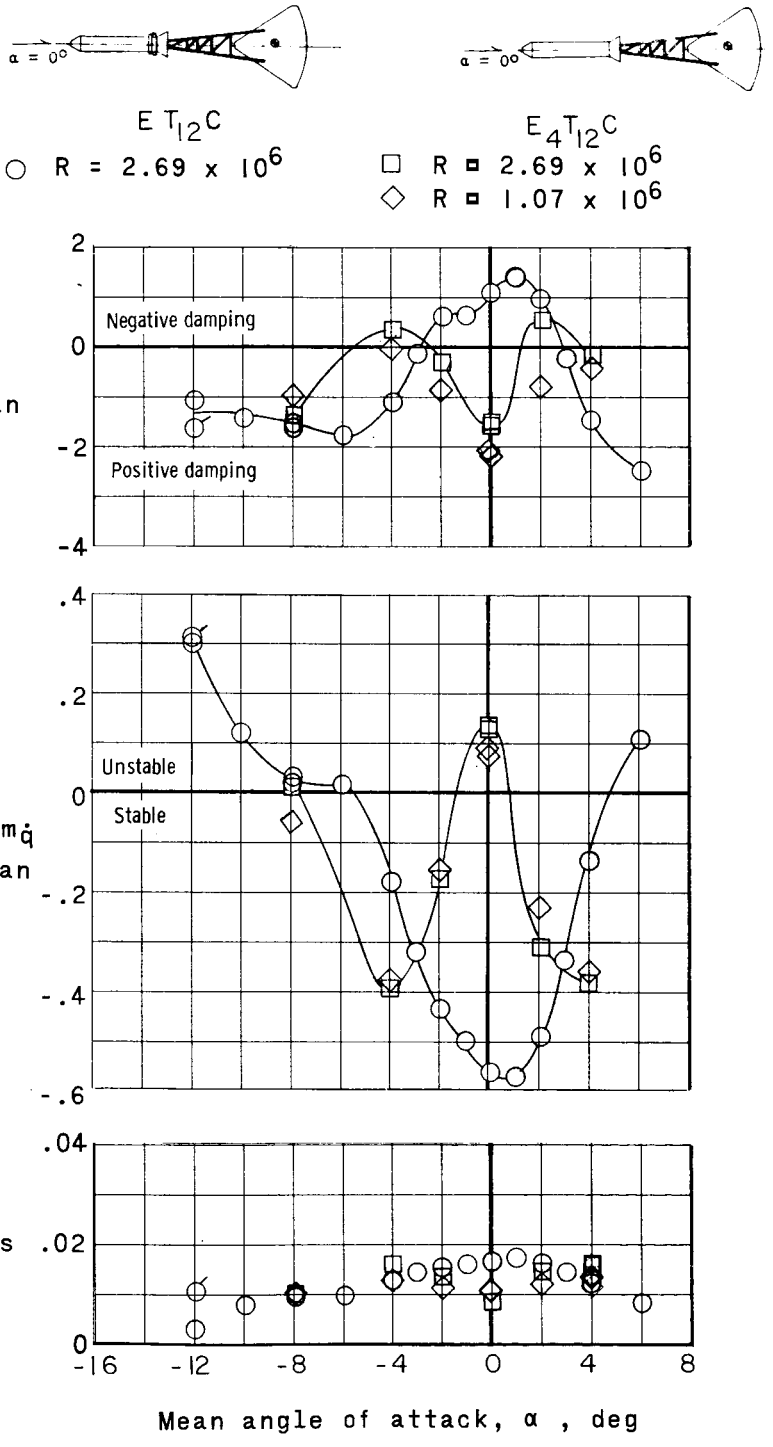

(d) M = 4.65.

Figure 3.- Concluded.

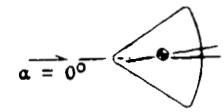

	M	R
○	2.40	1.58 x 10^6
□	2.98	1.68 x 10^6
◇	3.96	2.09 x 10^6
▽	4.65	2.69 x 10^6

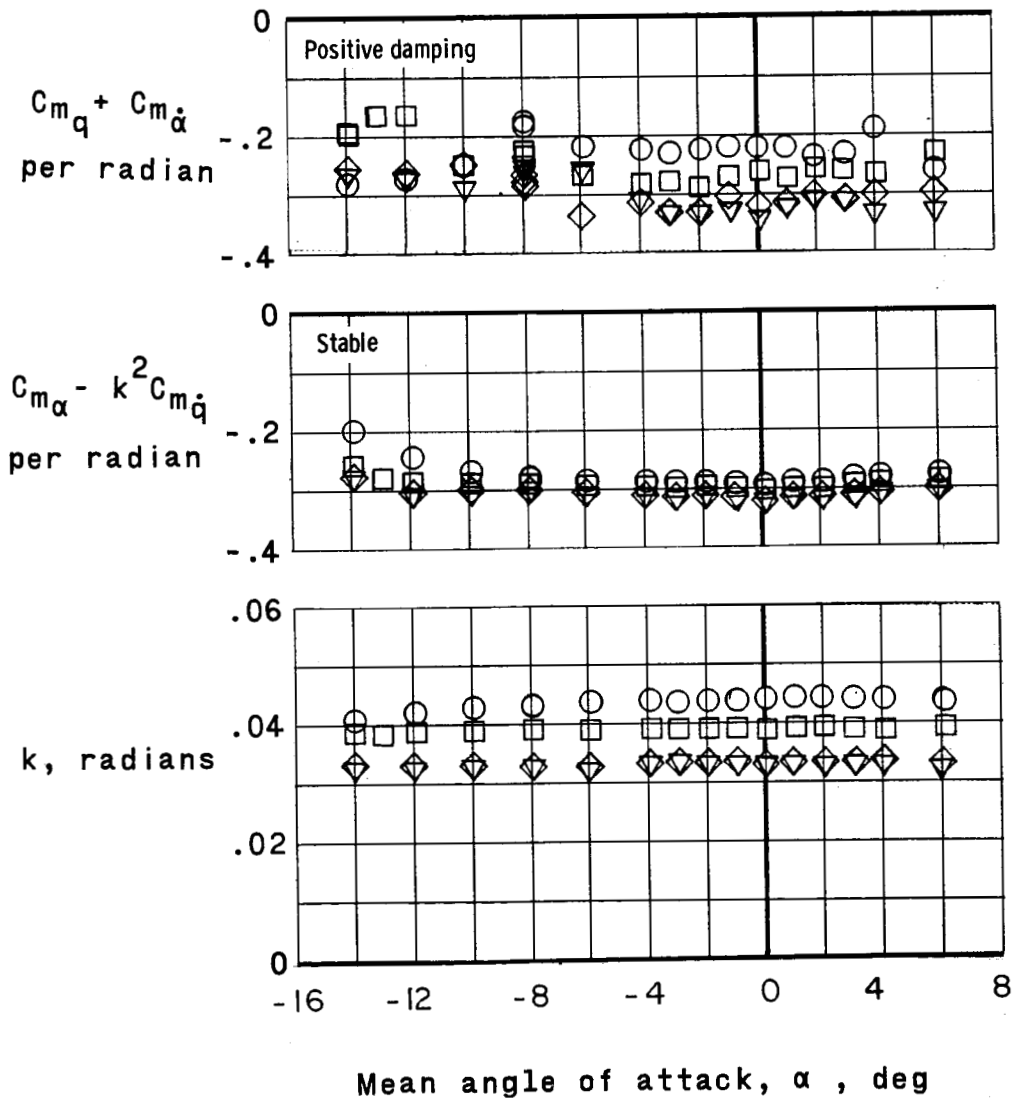

Figure 4.- Variation of damping-in-pitch parameter, oscillatory-longitudinal-stability parameter, and reduced-frequency parameter with angle of attack for model of command module C with heat shield aft.

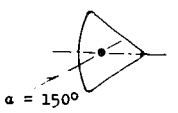

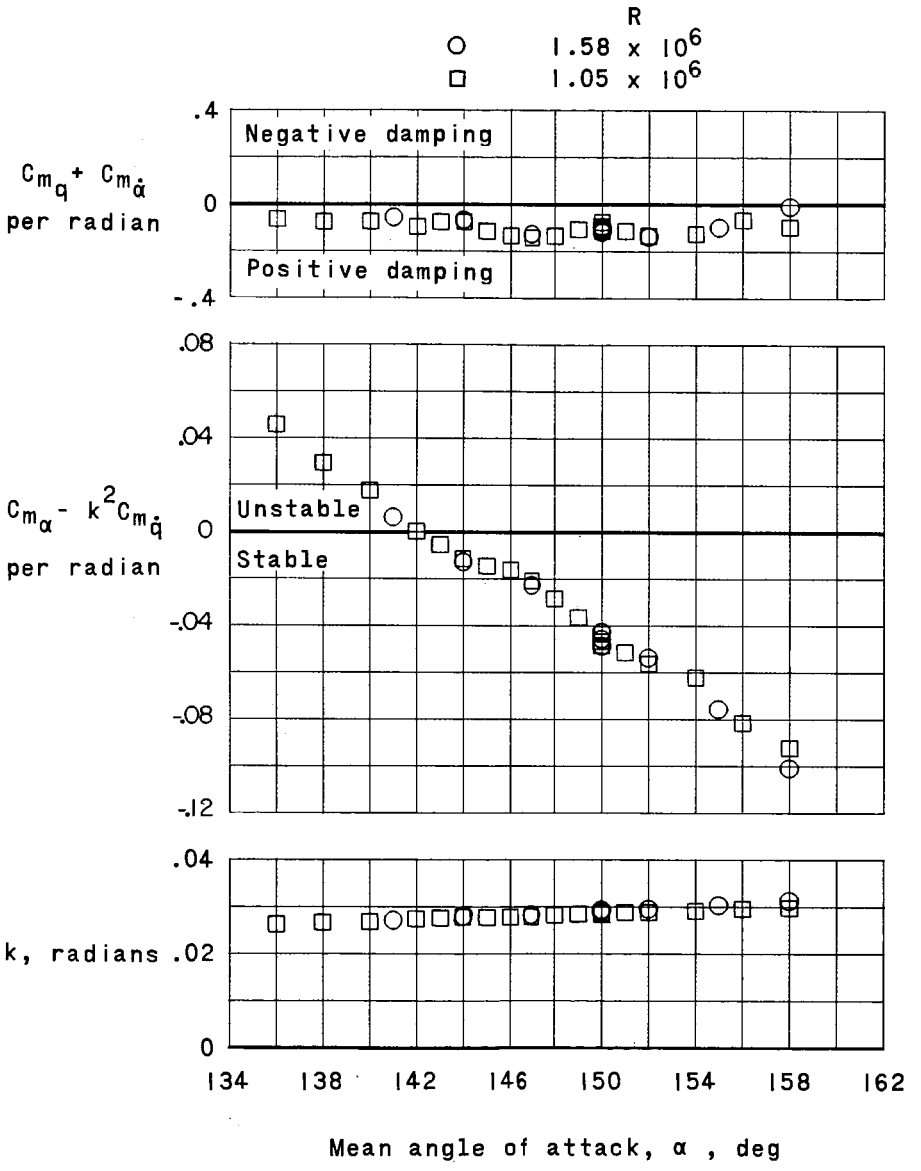

(a) M = 2.40.

Figure 5.- Variation of damping-in-pitch parameter, oscillatory-longitudinal-stability parameter, and reduced-frequency parameter with angle of attack for model of the command module C in reentry attitude.

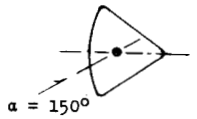

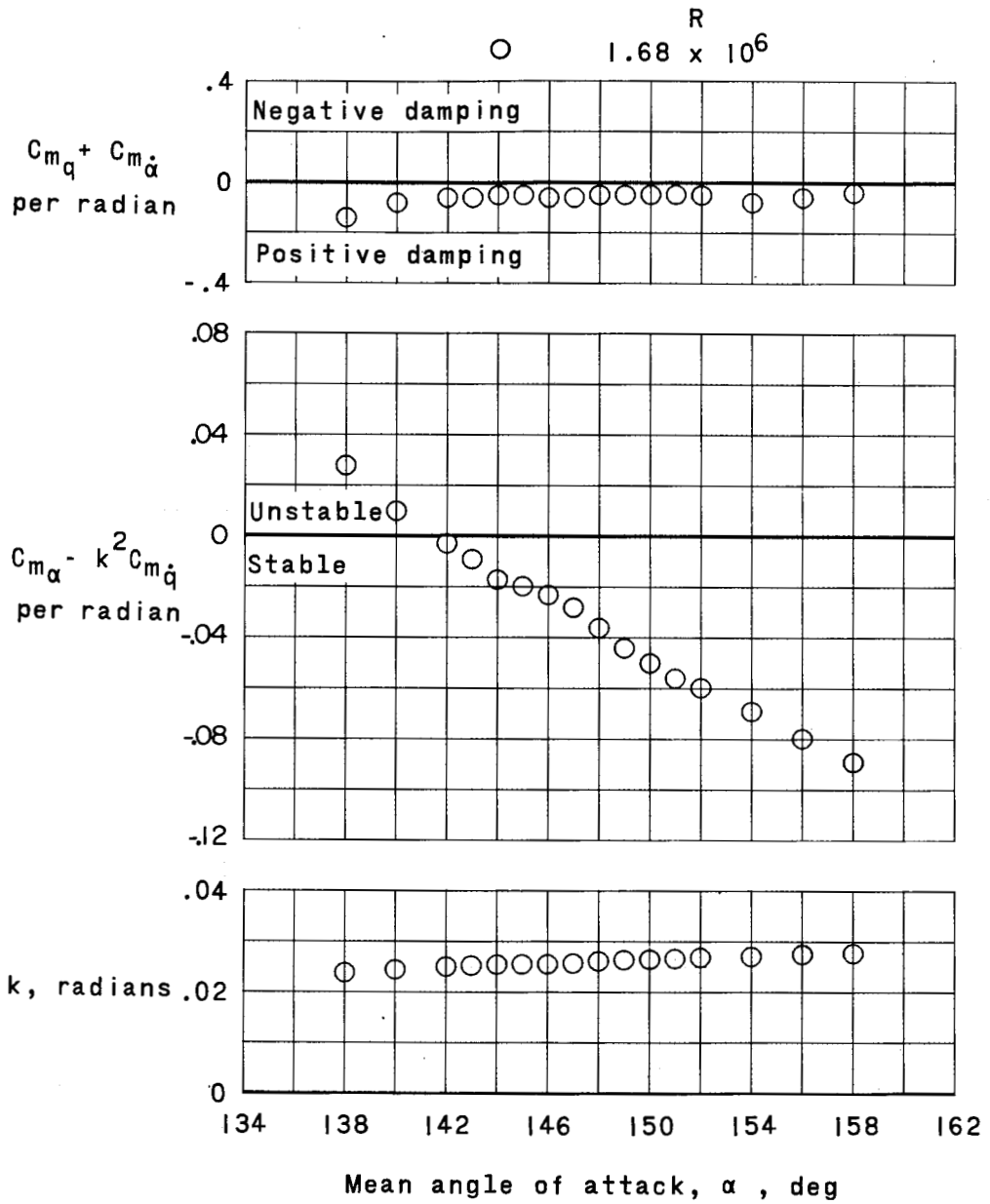

(b) M = 2.98.

Figure 5.- Continued.

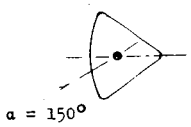

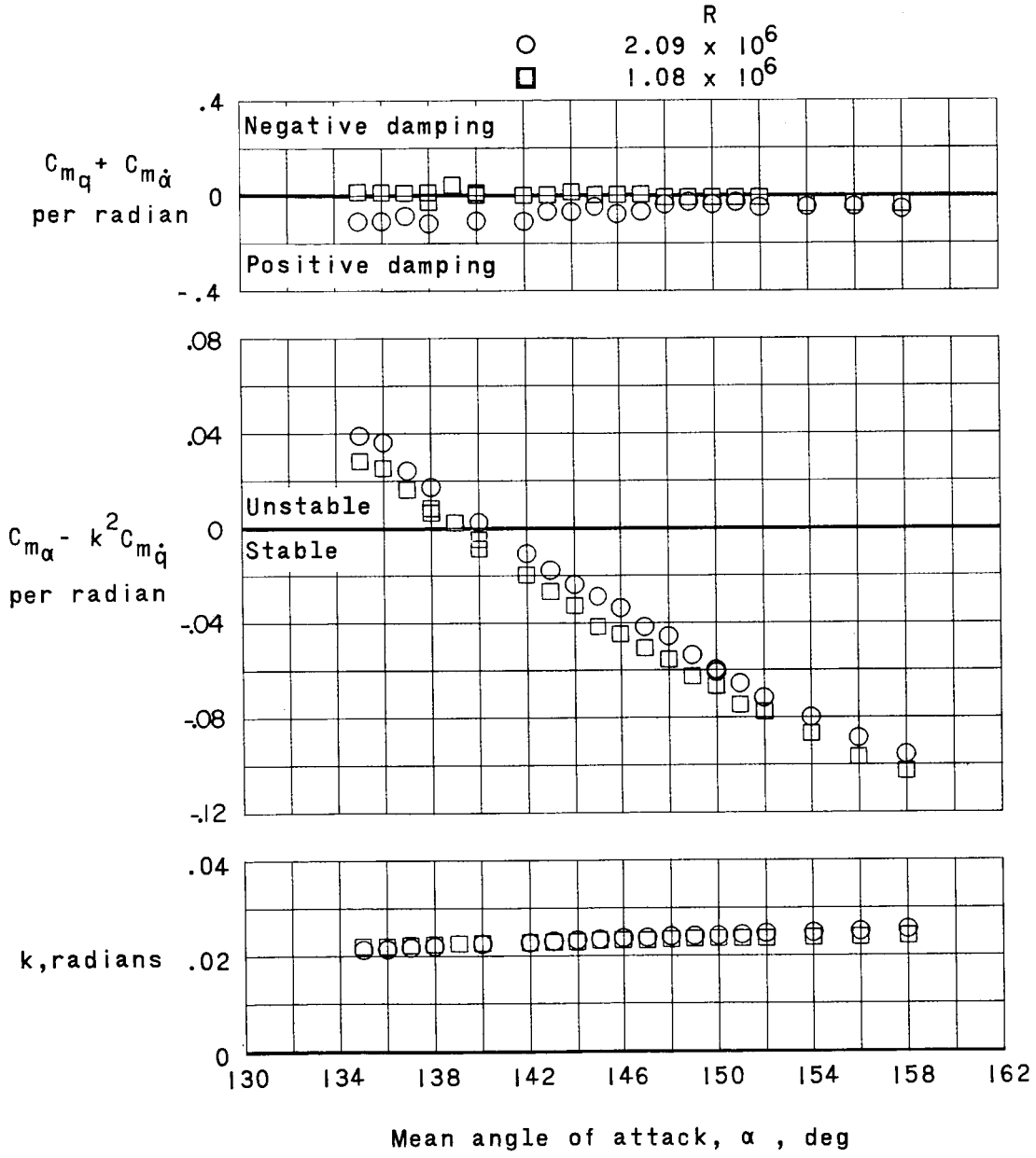

(c) M = 3.96.

Figure 5.- Continued.

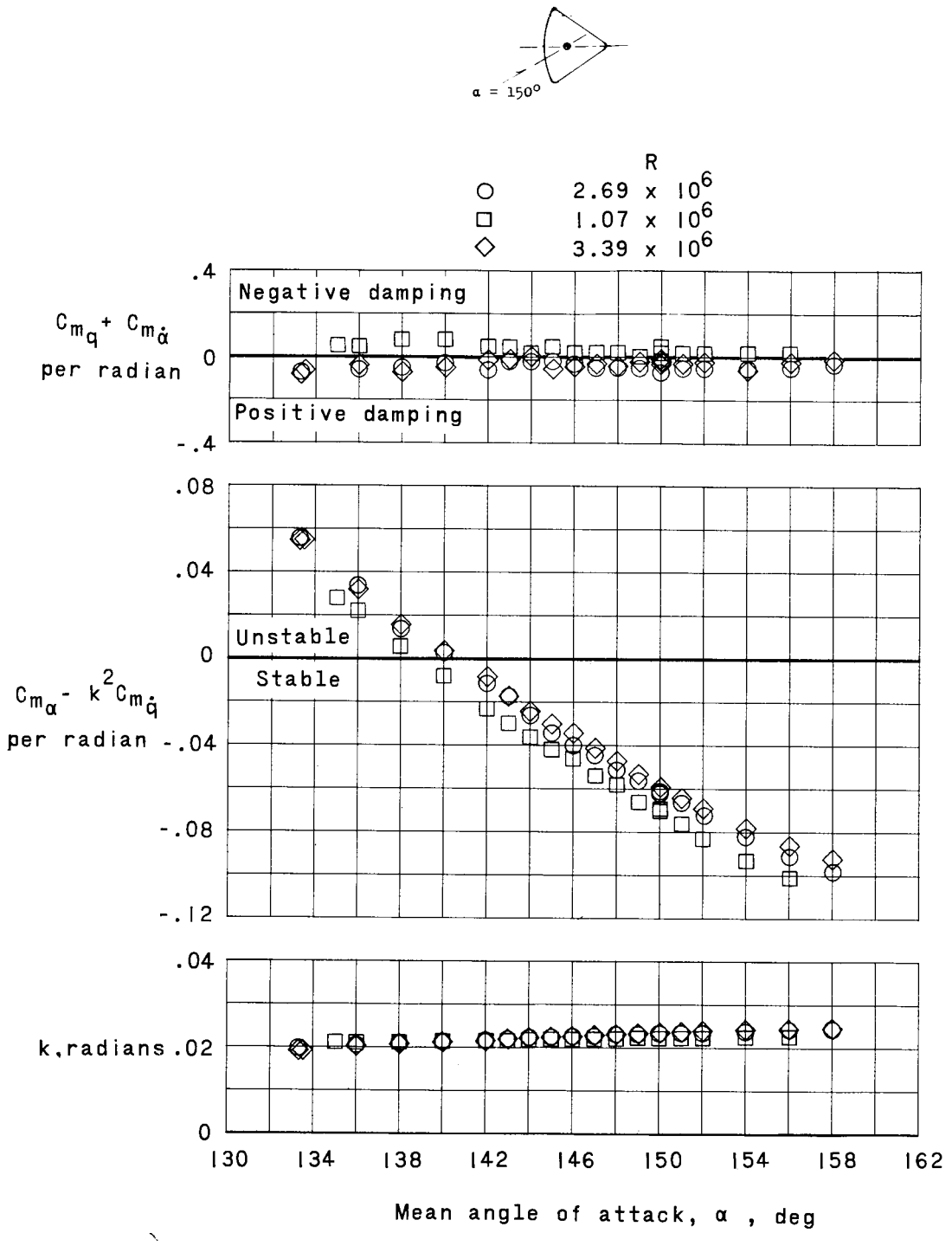

(d) M = 4.65.

Figure 5.- Concluded.

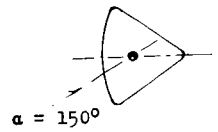

	M	R
○	2.40	1.58 x 10^6
□	2.98	1.68 x 10^6
◇	3.96	2.09 x 10^6
▽	4.65	2.69 x 10^6

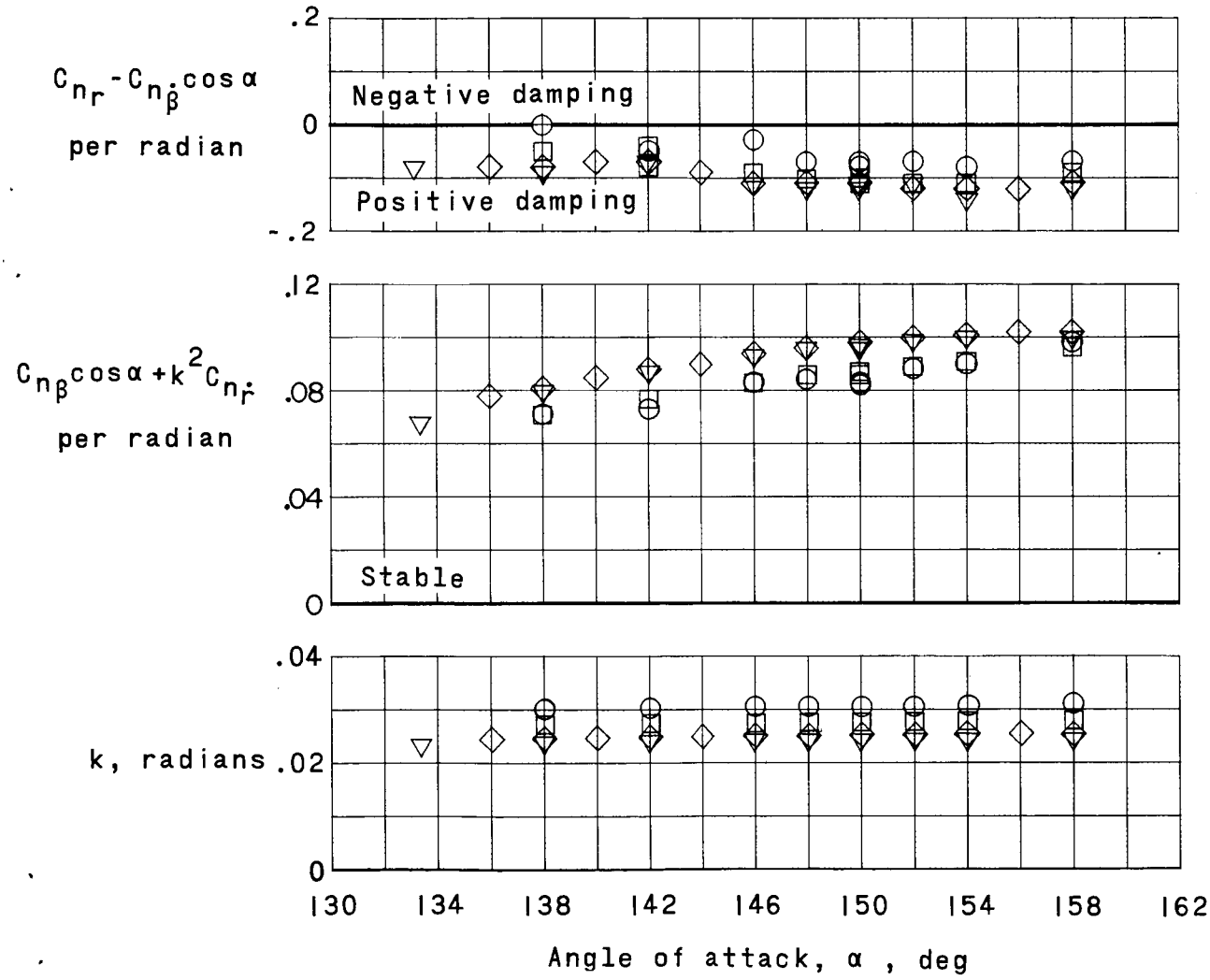

Figure 6.- Variation of damping-in-yaw parameter, oscillatory-directional-stability parameter, and reduced-frequency parameter with angle of attack for model of command module C in reentry attitude.

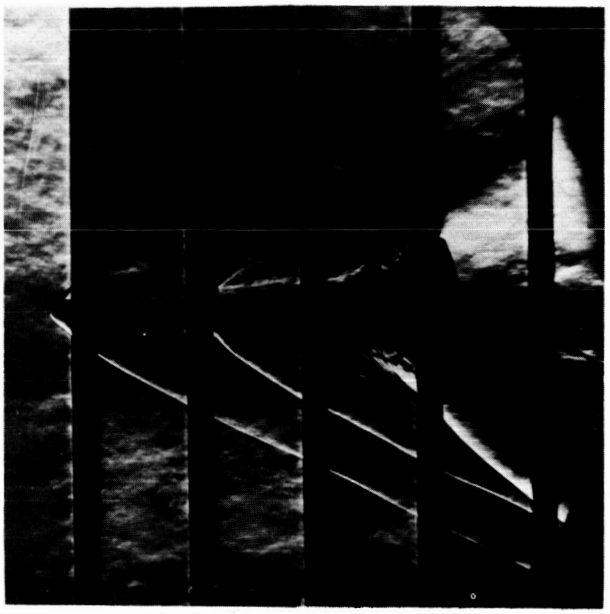

M = 2.40

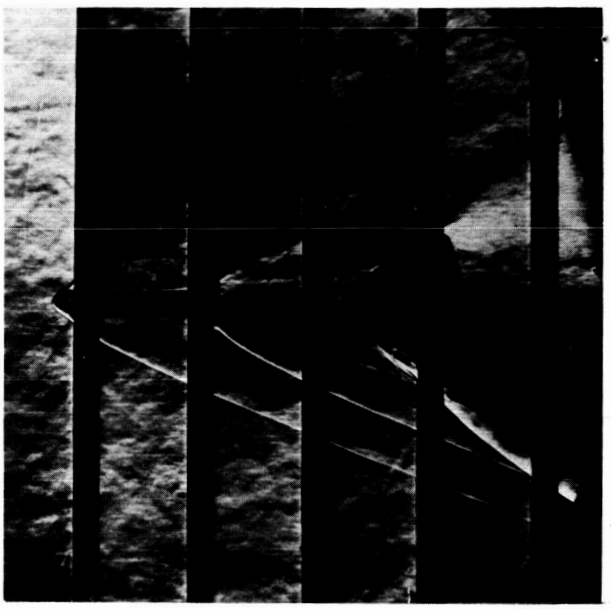

M = 2.98

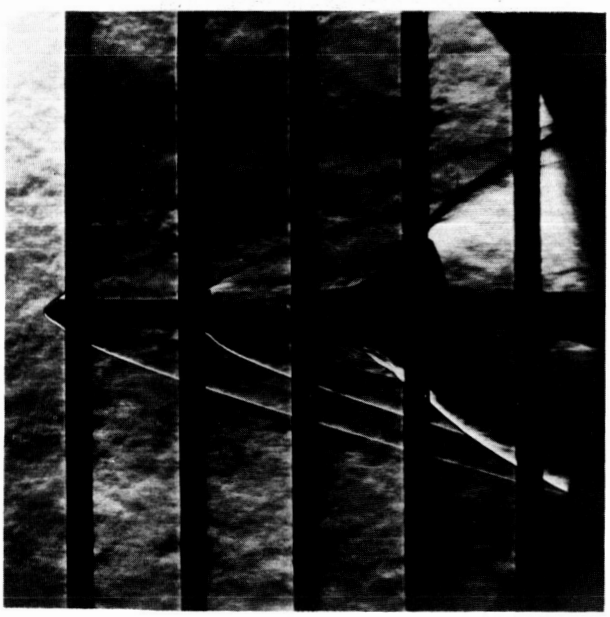

M = 3.96

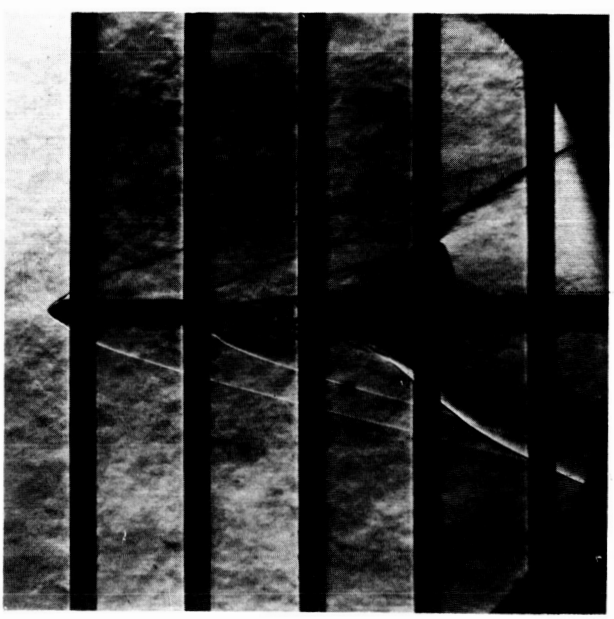

M = 4.65

L-62-7054

Figure 7.- Schlieren photographs of model of launch-escape configuration $E_4T_{12}C$, taken at an angle of attack of 0°.

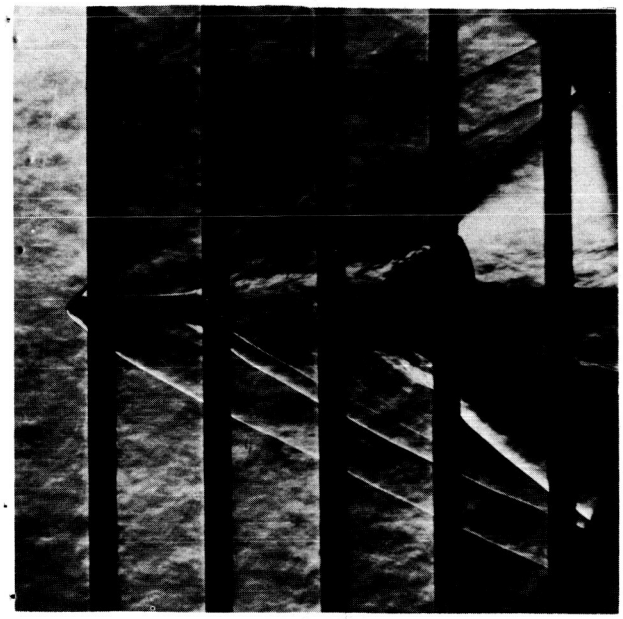

M = 2.40

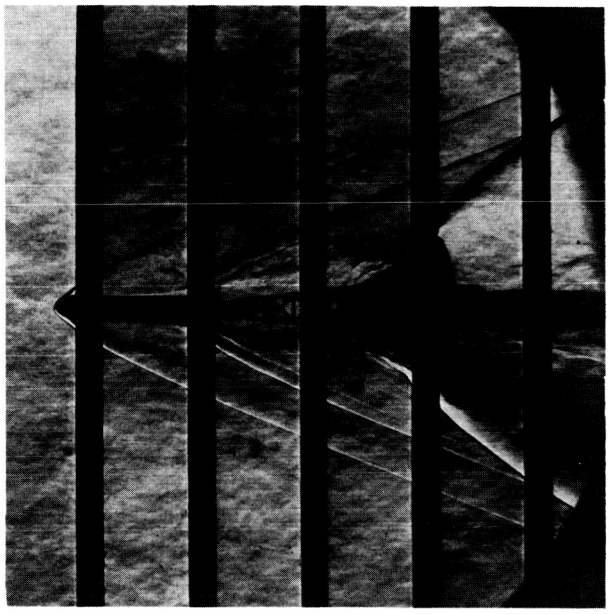

M = 2.98

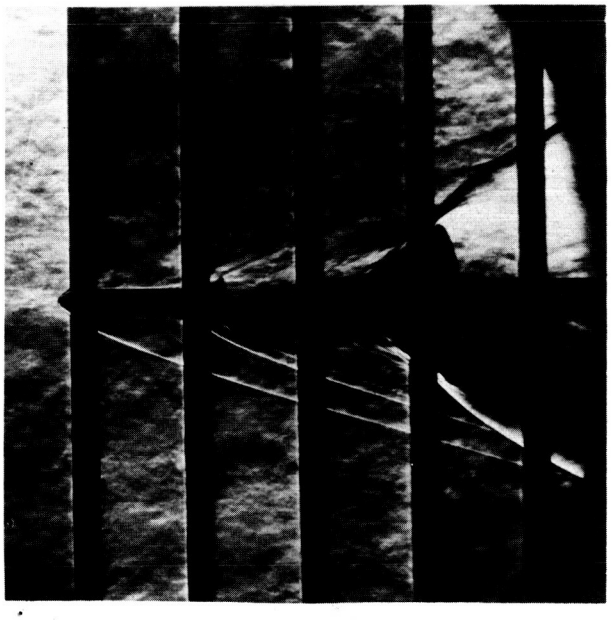

M = 3.96

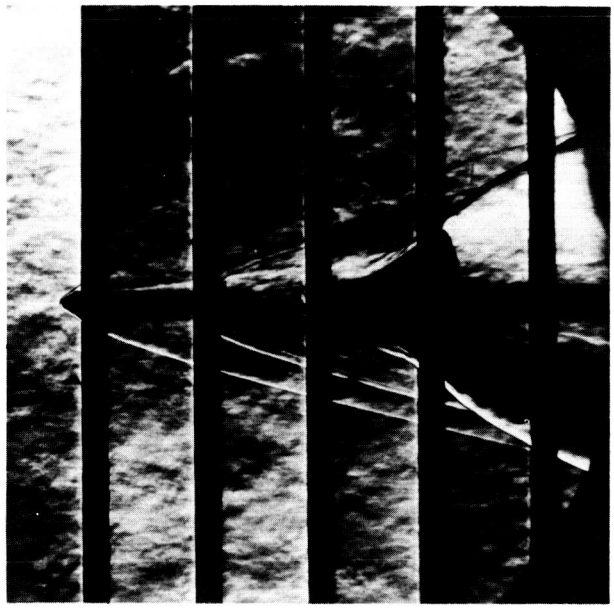

M = 4.65

L-62-7055

Figure 8.- Schlieren photographs of model of launch-escape configuration $ET_{12}C$, taken at an angle of attack of 0^{o}.

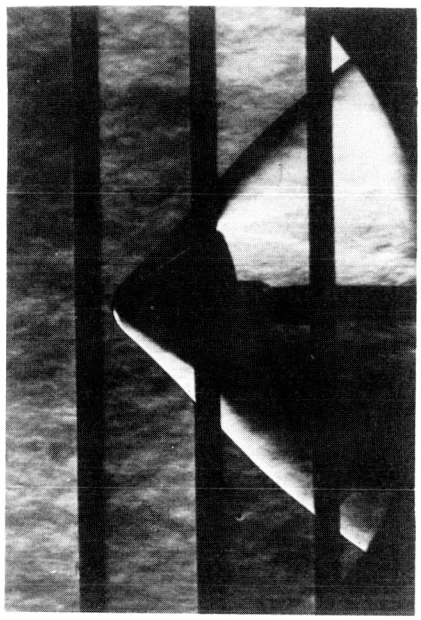

M = 2.40

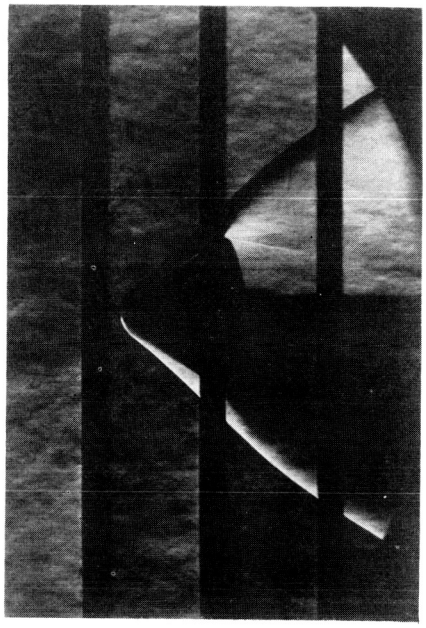

M = 2.98

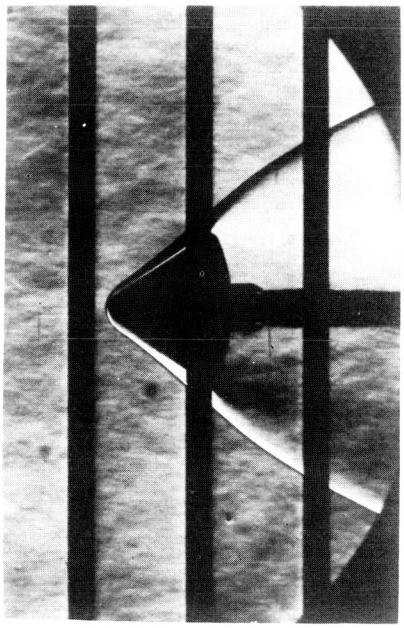

M = 3.96

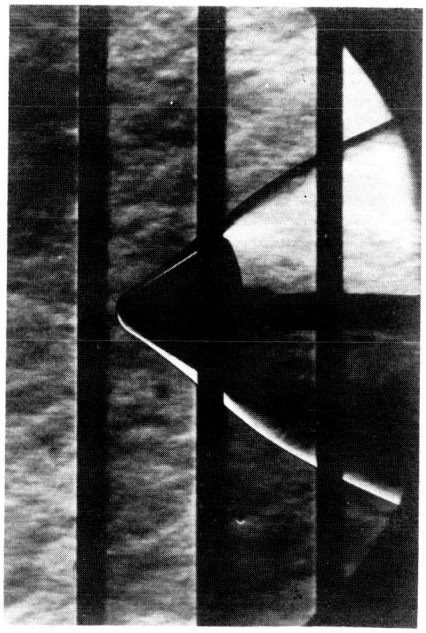

M = 4.65

L-62-7056

Figure 9.- Schlieren photographs of model of command module C with heat shield aft, taken at an angle of attack of 0°.

M = 2.40

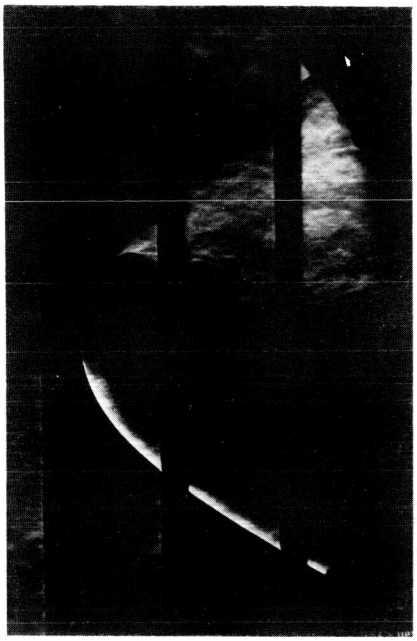

M = 2.98

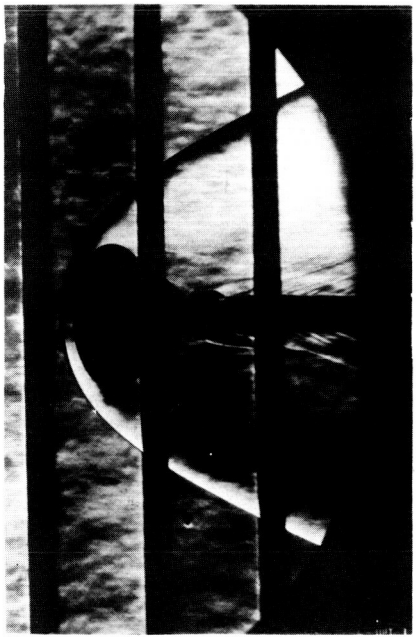

M = 3.96

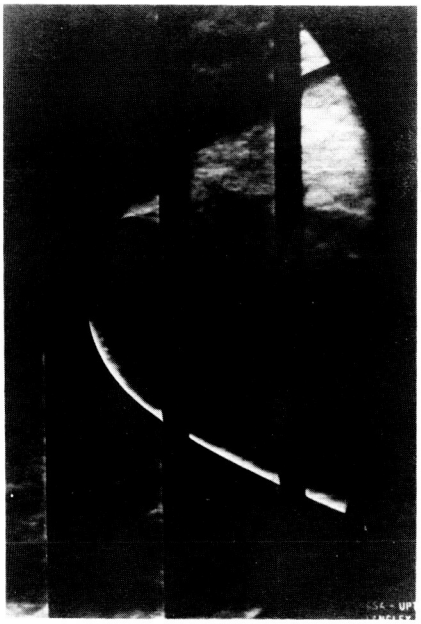

M = 4.65

L-62-7057

Figure 10.- Schlieren photographs of model of command module C in reentry attitude, taken at an angle of attack of 150°.